

Simulation and algorithmization of analysis of heat and mass transfer processes in chemical electrothermy units in non-ferrous metallurgy

S. V. Pancnehko, Doctor of Engineering Sciences, Professor, Department of Physics¹, e-mail: tan_pan@inbox.ru

M. I. Dli, Professor, Doctor of Engineering Sciences, Deputy Director for Science, Head of the Department of Information Technologies in Economics and Management¹, e-mail: midli@mail.ru

A. A. Bykov, Deputy Professor, Candidate of Pedagogical Sciences, Head of the Department of Physics¹, e-mail: alex1by@mail.ru

¹Branch of the National Research University "Moscow Power Engineering Institute", Smolensk, Russia.

Proposed is an algorithm for calculating heat and mass transfer in electrothermal ore recovery processes in non-ferrous metallurgy. To implement the algorithm, the finite element method was used, which allows to take into account complex configuration of the internal volume of the reactor. A finite element grid automatic construction algorithm was used. An iterative algorithm for the finite element equations implementation with the matrix width optimization and the use of symmetry properties is proposed.

A set of programs that allows to calculate operating modes of electrothermal ore-smelting reactors of any design, including those used in the smelting of non-ferrous metal alloys, has been developed. The interface of the programs is user-friendly. The multi-document interface provides visualization of the calculation results in the form of isolines of temperature fields and velocity vectors.

Keywords: electrothermal reactors, heat and mass transfer processes, iterative algorithm, finite element method, computer simulation, simulation of reduction processes in non-ferrous metallurgy.

DOI: 10.17580/nfm.2022.01.07

Introduction

Simulation of processes in electrothermal ore-smelting reactors for manufacturing non-ferrous metal alloys allows one to determine conditions for optimal functioning and cost reduction per unit of output [1–8]. There are not so many works that take the peculiarities of the physics of processes occurring in the reactors of this type into account [9–12].

Having regard to the analogy of processes in aggregates for the production of nickel, copper, phosphorus, calcium carbide, titanium carbide, etc., this approach acquires appropriate universality.

Such reactors are made as a closed or open-type bath, into which a charge, fluxes and reducing agent (coke) enter and where high-temperature heat and mass transfer processes are determining in the course of target reactions. Energy is supplied to the reaction zone by means of electrodes as Joule heat. The charge is fed into the melt bath through the lid on top, heated by filtered furnace gases in the countercurrent. The final charge heating up to the melting temperature and the melting process of the dispersed material itself occurs in the melt, as a rule [23]. The charge layer is above the layer of coke ejected by the melt. The coke zone is formed under the charge layer as the reducing agent enters the melt together with the charge. In that way, during the reactor operation, zones with different phase composition and properties are formed, where

take place the processes of charge heating and gas cooling (charge zone), melting (melting zone or melting front), reduction (coke zone), etc.

Mathematical model of heat and mass transfer

A model for describing energy exchange in an ore-smelting reactor of chemical electrothermics includes equations of electric potential distribution, equations of phase motion, equations of continuity, mass conservation, equations of energy and mass transfer. The use of the method proposed in [14] for determining the effective coefficients of thermal conductivity and diffusion in a gas-liquid medium makes it possible to reduce the system of equations of heat and mass transfer and hydrodynamics in the reaction zone to the equations of thermal conductivity and diffusion.

In this case, the electric potential φ_e distribution is determined from the following equation:

$$\operatorname{div}((1/\rho_e)\operatorname{grad}\varphi_e) = 0. \quad (1)$$

The equations of the energy and mass transfer in the reaction and slag zone of an electrothermal ore-smelting reactor can be written as follows:

$$\operatorname{div}(\lambda_T \operatorname{grad} T_p) + q_{ve} - q_{cr} \omega_{cr} = 0, \quad (2)$$

$$\operatorname{div}(D_T \operatorname{grad} C_p) - \omega_{cr} = 0. \quad (3)$$

Heat exchange in the charge zone of the reactor is determined by energy transfer equations in the approximation

of interpenetrating components, kinematic equation for the motion of dispersed material and filtration equation in the Darcy's approximation:

$$(1 - \varepsilon)c_m \rho_m v_m \text{grad} T_m - \text{div}(\lambda_m \text{grad} T_m) = \alpha_v (T_g - T_m), \quad (4)$$

$$\varepsilon c_g \rho_g v_g \nabla T_g - \text{div}(\lambda_g \text{grad} T_g) = \alpha_v (T_m - T_g), \quad (5)$$

$$\text{div}(\text{grad} \varphi_m) = 0, v_m = -\text{grad} \varphi_m, \quad (6)$$

$$\text{div}(k \text{grad} \varphi_g) = \gamma \omega_{cr}, v_g = -k \text{grad} \varphi_g, \quad (7)$$

where T_f is the melt temperature; C_f is the reagent concentration; λ_T is the effective turbulent thermal conductivity of the melt caused by bubbling with the reduction reaction gaseous products; q_{cr} is thermal effect of the endothermic reduction reaction; D_T is an effective coefficient of turbulent diffusion; T_m, T_g are the charge and furnace gas temperatures; φ_g, φ_m are potential functions for describing gas filtration in the dispersed charge layer and gravitational motion of dispersed particles; $\rho_m, \rho_g, c_m, c_g, \lambda_m, \lambda_g$ are density, heat capacity and thermal conductivity of charge material and gas, respectively, v_m, v_g are the charge and gas flow rates; $\gamma \omega_{cr}$ is the source of the gas mass resulting from the melting reaction, $k = k_0/\mu$ is a filtration coefficient ($k_0 = 6.15 \times 10^{-4} d_m^2$ is a permeability coefficient for randomly stacked balls; μ is the dynamic gas viscosity); α_v is a volumetric coefficient of heat transfer between the gas and charge, which is determined by the formula $\alpha_v = \alpha f$, where $f = 6/d_c$ is the specific surface area of charge particles; d_m is the equivalent diameter of charge particles; α is a heat transfer coefficient.

$\omega_{cr} = S_\kappa K_0 \exp(-E/RT) C_f$ is the chemical reduction reaction rate; S_κ is the specific surface of reducing agent (coke) particles; K_0 is a pre-exponential multiplier of the rate constant of the chemical reduction reaction; $q_{ve} = (1/\rho_e)(\text{grad} \varphi_e)^2$ is the power of heat-evolution per volume unit, where φ_e is the potential generated by electrodes, ρ_e is specific electrical resistance.

Boundary conditions at the melting front:

$$\Gamma \in \Gamma_{melt}, T_f = T_{melt} \quad (8)$$

Heat transfer through the lining:

$$\Gamma \in \Gamma_w, \lambda_T = \frac{\partial T_f}{\partial n} = -k_{he}(T_f - T_0) \quad (9)$$

Boundary conditions for the mass transfer equation at the melting front:

$$\Gamma \in \Gamma_{melt}, C = C_m, \quad (10)$$

The condition for walls (impermeability):

$$\Gamma \in \Gamma_w, \frac{\partial C_f}{\partial n} = 0, \quad (11)$$

Boundary conditions for electric potential

$$\text{on the bottom: } \Gamma \in \Gamma_d, \varphi_e = 0, \quad (12)$$

$$\text{on the electrode surface: } \Gamma \in \Gamma_e, \varphi_e = \varphi_{ee}, \quad (13)$$

$$\text{at the melt-charge boundary: } \Gamma \in \Gamma_{melt}, \frac{\partial \varphi_e}{\partial n} = 0, \quad (14)$$

at the interface of the k -th and $(k + 1)$ st current-conductive zones of the melt:

$$\Gamma \in \Gamma_{k, k+1}, \varphi_{ek} = \varphi_{ek+1}$$

$$\text{and } \frac{1}{\rho_{ek}} \frac{\partial \varphi_{ek}}{\partial n} = \frac{1}{\rho_{ek+1}} \frac{\partial \varphi_{ek+1}}{\partial n} \quad (15)$$

$$\text{Boundary conditions for the charge temperature at the upper boundary: } \Gamma \in \Gamma_m, T_m = T_{env}, \quad (16)$$

$$\text{at the melting front: } \Gamma \in \Gamma_{melt}, T_m = T_{melt} \quad (17)$$

$$\text{The gas temperature at the reaction zone outlet: } T_g = T_f, \quad (18)$$

Conditions at the melting front that determine the charge descent rate:

$$\Gamma \in \Gamma_{melt}, \frac{\partial \varphi_m}{\partial n} = - \left(\lambda_T \frac{\partial T_f}{\partial n} - \lambda_m \frac{\partial T_m}{\partial n} \right) \frac{1}{(\rho_m Q_{melt})} \quad (19)$$

Boundary conditions on walls (impermeability):

$$\Gamma \in \Gamma_w, \frac{\partial \varphi_m}{\partial n} = 0. \quad (20)$$

where T_{melt} is the charge melting point; T_0 is the temperature of the water cooling the reactor jacket; T_{env} is the charge zone upper boundary temperature equal to ambient temperature; k_{he} is a heat transfer coefficient. C_m is the reagent concentration in the charge; ρ_m is a bulk density of the charge material; Q_{melt} is the charge melting heat.

To indicate the boundaries, we have: Γ_m is the upper charge boundary; Γ_{melt} is the melting front; Γ_w are the walls of the reactor bath; Γ_d is the bottom; Γ_e is the surface of electrodes; $\Gamma_{k, k+1}$ are the interfaces of the k -th and $(k + 1)$ st current-conductive zones of the melt.

An important feature of the model is the interrelationship consideration of processes in the zones of different phase composition by including into the melting process model, which made it possible to identify the feed of raw materials into the reaction zone depending on a heat-hydraulic regime in the reactor volume.

The model allows to describe regularities of the influence of processes in the reaction zone on changes in the temperature of furnace gases in the underroof space when exposed to control parameters such as coke dosage, voltage on the electrodes, the charge granulo-metric composition and its composition, makes it possible to estimate the impact on the operating parameters of the furnace.

Method for implementing the mathematical model

The algorithm of the finite element method with automatic partitioning of the solution domain, performed in the C++ programming language, has been used for computer implementation of this mathematical model.

The calculation results are the fields of electric potential distribution, specific energy-release, material temperature, gas temperature, reagent concentration in the reaction zone. In addition, guaranteed is the possibility to display thermophysical parameters and values of integral characteristics of its operating mode, such as active electrical power, gas output, and consumption of individual charge components, average and maximum gas outlet temperatures.

The finite element method uses elements of a quadrangular shape with basic functions with first-order continuity, since they are most preferable for solving the equations of convective heat transfer [15].

The sought continuous quantity in the area of a quadrangular finite element is represented as

$$\Phi = \sum_{i=1}^4 N_i \Phi_i = [N][\Phi], \quad (21)$$

where Φ_i are the unknown values of the sought quantity at the finite element nodes, N_i are the basic functions of the element. A local coordinate system (ξ, η) is introduced on the finite element, where $-1 \leq \xi \leq 1, -1 \leq \eta \leq 1$, which allows to use complex shapes, and also simplifies the integration of equations. The transformation of this system into a Cartesian coordinate system (x, y) looks like this

$$\begin{aligned} x &= \sum_{i=1}^4 N_i(\xi, \eta) x_i = [N][x], \\ y &= \sum_{i=1}^4 N_i(\xi, \eta) y_i = [N][y], \end{aligned} \quad (22)$$

where x_i and y_i are the coordinates of the finite element nodes.

The basic functions of an element with the use of a local coordinate system have the form as follows:

$$\begin{aligned} N_1 &= \frac{1}{4} (1 - \xi)(1 - \eta); \quad N_2 = \frac{1}{4} (1 + \xi)(1 - \eta); \\ N_3 &= \frac{1}{4} (1 + \xi)(1 + \eta); \quad N_4 = \frac{1}{4} (1 - \xi)(1 + \eta). \end{aligned} \quad (23)$$

To calculate the derivatives in coordinates (ξ, η) , the following ratio is used:

$$\begin{bmatrix} \frac{\partial \Phi}{\partial \xi} \\ \frac{\partial \Phi}{\partial \eta} \end{bmatrix} = [J] \begin{bmatrix} \frac{\partial \Phi}{\partial x} \\ \frac{\partial \Phi}{\partial y} \end{bmatrix}, \quad (24)$$

where the Jacobian $[J]$ is calculated by the formula

$$[J] = \begin{bmatrix} \frac{\partial x}{\partial \xi} & \frac{\partial y}{\partial \xi} \\ \frac{\partial x}{\partial \eta} & \frac{\partial y}{\partial \eta} \end{bmatrix}. \quad (25)$$

To solve differential equations, the Galerkin method is used together with the finite element method. It implies that the desired solution will be the best if it is based on the orthogonality requirement of residual and basis functions:

$$\int_S L(\Phi)[N] \partial x \partial y = 0, \quad (26)$$

where $L(x) = 0$ is an integrable differential equation.

Numerical integration using the Newton–Cotes quadrature formulas in the local coordinates of the element is used to calculate integrals:

$$\int_S (\xi, \eta) \partial x \partial y = \det[J] \sum_{k=1}^n H_k f(\xi_k, \eta_k), \quad (27)$$

where $n = 4$ is the number of integration points, $H_k = 1$ are the weighting factors given for the points with local coordinates $\xi_k = \pm 0,577350, \eta_k = \pm 0,577350, f$ is the integrable function. The systems of equations obtained because of integration for each element are combined into a united system of equations for the entire domain.

To generate a finite element grid, the superelement method is used when an irregular grid of curved 8-node quadrangles is used in the initial area, which are called superelements S with nodes $P_i = P(x_i^s, y_i^s), I = 1, 2, \dots, 8$. Using the following mapping

$$x(\xi, \eta) = x_i^s N_i(\xi, \eta), \quad y(\xi, \eta) = y_i^s N_i(\xi, \eta), \quad (28)$$

the square Q is converted into a curved superelement S , where $N_i(\xi, \eta)$ are quadratic basis functions on the superelement

$$N_1 = -\frac{1}{4} (1 - \xi)(1 - \eta)(\xi + \eta + 1)$$

$$N_2 = \frac{1}{2} (1 - \xi^2)(1 - \eta)$$

$$N_3 = \frac{1}{4} (1 + \xi)(1 - \eta)(\xi - \eta - 1)$$

$$N_4 = \frac{1}{2} (1 + \xi)(1 - \eta^2)$$

$$N_5 = \frac{1}{4} (1 + \xi)(1 + \eta)(\xi + \eta - 1)$$

$$N_6 = \frac{1}{2} (1 - \xi^2)(1 + \eta)$$

$$N_7 = -\frac{1}{4} (1 - \xi)(1 + \eta)(\xi - \eta + 1)$$

$$N_8 = \frac{1}{2} (1 - \xi)(1 - \eta^2). \tag{29}$$

The uniform grid constructed in Q is mapped to the curved grid of the superelement S . At the same time, the location of P_i nodal points on the sides allows to fulfill local closeness of the grid. Uniting the grids constructed in this way on each superelement gives a grid over the entire source area.

For example, Fig. 1 shows a grid of quadrangular finite elements generated for the model of an electrothermal ore-smelting reactor. At that, the boundaries of superelements were selected at the boundaries of the calculated zones. The boundaries of electrodes were approximated by a parabola.

The equations of the mathematical model of the reactor can be reduced to the following two forms:

$$\text{div}(k \cdot \text{grad } \Phi) - q = 0; \tag{30}$$

$$V \cdot \text{grad } \Phi - \text{div}(k \cdot \text{grad } \Phi) + q = 0. \tag{31}$$

The system of linear equations corresponding to these equations on a finite element is represented as follows:

$$[A][\Phi] = [F], \tag{32}$$

where $[A]$ is the matrix of the system of equations, $[F]$ is the vector of absolute terms.

Using the representation of Φ by means of basis functions, the Green's theorem for order reduction and quadrature formulas for numerical integration, the matrix of the system of equations for equation (32) is defined as

$$[A] = \det[J] \sum_{k=0}^n [B]^T [K] [B], \tag{33}$$

where $[B] = \begin{bmatrix} \frac{\partial [M]}{\partial x} \\ \frac{\partial [M]}{\partial y} \end{bmatrix}$ is the matrix of derivative functions of

the form, $[K] = [k \ 0 \ 0 \ k]$ is the matrix of properties, $[F] = q \cdot \det[J] \sum_{k=0}^n [N]^T$ is the vector of absolute terms.

In this case, the matrices are determined at the corresponding points (ξ_k, η_k) of the finite element.

To approximate equations of type (31) at large values of V/k ratio, the Petrov-Galerkin method is used, which is a finite element analogue of the finite difference method with upstream differences. At that, functions other than the basic one (the so-called asymmetric weighting functions) are used as weighting functions. In this case, the condition of the best solution takes the form as follows:

$$\int_S [L(\Phi)[W] \partial x \partial y = 0, \tag{34}$$

here $[W]$ is a vector of asymmetric weighting functions, taken in the following form:

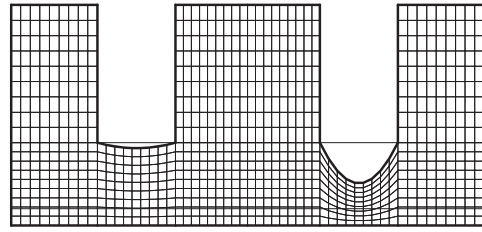


Fig. 1. Grid of finite quadrangular finite elements

$$W_1 = \frac{1}{4} (1 - \xi)(1 + 1.5\alpha_{12}(1 + \xi))(1 - \eta)(1 + 1.5\alpha_{14}(1 + \eta)),$$

$$W_2 = \frac{1}{4} (1 + \xi)(1 - 1.5\alpha_{12}(1 - \xi))(1 - \eta)(1 + 1.5\alpha_{23}(1 + \eta)),$$

$$W_3 = \frac{1}{4} (1 + \xi)(1 - 1.5\alpha_{34}(1 - \xi))(1 + \eta)(1 - 1.5\alpha_{23}(1 + \eta)),$$

$$W_4 = \frac{1}{4} (1 - \xi)(1 + 1.5\alpha_{34}(1 + \xi))(1 + \eta)(1 - 1.5\alpha_{14}(1 - \eta)), \tag{35}$$

where α_{ij} are the coefficients determining the degree of asymmetry (the indexes define the numbers of the finite element nodes connected by corresponding sides), the optimal value of which is determined from the following expression:

$$\alpha_{ij} = \frac{\exp\left(\frac{Pe}{2}\right) + \exp\left(-\frac{Pe}{2}\right)}{\exp\left(\frac{Pe}{2}\right) - \exp\left(-\frac{Pe}{2}\right)} - \frac{2}{Pe},$$

$$Pe = \frac{h_{ij} V_{av}}{2k}, \quad V_{av} = \frac{V_i + V_j}{2} \tag{36}$$

where Pe is the Péclet grid number; h_{ij} is the length of the finite element side connecting the nodes i, j ; V_{av} is the average speed along this side; V_i and V_j are the velocity vector values at nodes i and j ; I_{ij} is the direction vector of the side ij .

When using asymmetric basis functions, the matrix of a system of linear equations approximating a differential equation of type (31) will be defined as follows:

$$[A] = \det[J] \sum_{k=0}^n [W]^T [V] [B] + [D]^T [K] [B], \tag{37}$$

where $[D] = \begin{bmatrix} \frac{\partial [W]}{\partial x} \\ \frac{\partial [W]}{\partial y} \end{bmatrix}$ is the matrix of derivative functions

of the form, $[V]$ is the velocity vector.

$$[F] = q \cdot \det[J] \sum_{k=0}^n [W]^T \tag{38}$$

is a vector of free members.

The resulting matrix of combined equations in the finite element method is sparse (banded). Over a long period, direct methods such as the Gaussian elimination method with the choice of an exclusionary element and taking into account matrix sparsity and banded structure have been used to solve the equations sets of this type [15–17]. At the same time, much attention has been paid to the use of algorithms for renumbering grid nodes, which reduce both the amount of computer memory needed to store the matrix and the calculation time [17–18].

Matrices of combined linear equations approximating differential diffusion equations (equations of type (30)) are symmetric and positive-definite; they are well solved by direct methods. In contrast to them, matrices of the systems approximating differential equations with convective terms (equations of type (31)) do not have a regular structure, are asymmetric and poorly conditioned, which limits the use of direct methods for solving such systems. To eliminate the difficulties associated with increasing the dimension of equations sets, it is necessary to use iteration methods.

To implement the method of solving simultaneous equations, one can use the method of adjoint gradient, which is characterized by high convergence and does not require setting iterative parameters. This method is adapted for solving symmetric positive-definite systems of algebraic equations [19–20] and its generalization, the induced dimension reduction (IDR) method, is suitable for both non-symmetric and non-positively definite equations sets [21]. The algorithm of the adjoint gradient method (IDR) for solving equations sets of $[A][X] = [B]$ form is given below.

The initial approximation $[X]_0$ and calculation accuracy ε are specified;

$$[F]_0 = [A][X]_0 - [B]; [dG]_0 = [dY]_0 = 0;$$

$$n = n + 1;$$

$$[S]_n = [F]_{n-1} + w_{n-1} [dG]_{n-1}; [T]_n = [A][S]_n;$$

$$\text{If } n = 1 \text{ or } n \text{ is even } \alpha_n = \frac{([T]_n[S]_n)}{([T]_n[T]_n)}, \text{ go to step 7;}$$

$$\alpha_n = \alpha_{n-1};$$

$$[dX]_n = w_{n-1} [dY]_{n-1} - \alpha_n [S]_n;$$

$$[dF]_n = w_{n-1} [dG]_{n-1} - \alpha_n [T]_n;$$

$$[X]_n = [X]_{n-1} + [dX]_n; [F]_n = [F]_{n-1} + [dF]_n;$$

If n is even $[dG]_n = [dG]_{n-1}; [dY]_n = [dY]_{n-1}$; go to step 12;

$$[dG]_n = [dF]_n; [dY]_n = [dX]_n;$$

$$W_n = - \frac{([F]_n[dF]_n)}{([F]_n[dG]_n)};$$

$$\text{If } \frac{|[dX]_n|}{|[X]_n|} > \varepsilon, \text{ go to step 3;}$$

The end of the calculation with the result $[X]_n$.

Sets of algebraic equations of the finite element method, as already noted above, have a banded structure. The time of their solution is $T \sim \beta^2 N$, and the amount of computer memory required to store the matrix is $V \sim \beta N$, where N is a number of unknown quantities, β is the band width [21–22]. The value of β depends on the numbering of grid nodes and can assume values in a wide range $\sqrt{N} \leq \beta < N$.

In this paper, when storing the matrix of simultaneous equations, almost all zero (insignificant) coefficients are excluded. This is achieved by using two one-dimensional arrays, one of which stores real values of the coefficients of equations, and the other contains integer numbers of variables corresponding to these coefficients. For quadrangular bilinear finite elements, the number of nodes adjacent to a given node does not exceed eight.

Thus, this method of storing the matrix of simultaneous equations is equivalent to the traditional one with a band width equal to nine, which allows significantly shorten the calculation time along with reducing the information amount. Arrays for storing the equations set coefficients and numbers of the corresponding variables have dimension $N \times M$, where M is the maximum number of variables appearing in the equation. The algorithm for calculating vector $[F] = [A][X]$ using the proposed method of storing the matrix $[A]$ is given below. It is assumed that the matrix coefficients are stored in the array Matr, and the numbers of the corresponding variables in the array Index.

Algorithm for the vector $[F] = [A][X]$ calculation

```
for(i=0; i<N; i++) {
  F[i]=0;
  for(j=0; j<M; j++) {
    F[i]+=Matr[i*M+j]*X[Index[i*M+j]];
  }
}
```

A two-dimensional mathematical model is used to simulate the processes in an electrothermal ore-smelting reactor. In this case, the sections passing through the centers of two electrodes are considered. The calculation of heat and mass exchange is reduced to solving a system of differential equations.

The heat transfer equation in the reaction zone of the furnace, which determines the temperature distribution, is nonlinear, due to the exponential dependence of the reduction reaction rate on temperature. The convergence of a system that includes such an equation depends on correct choice of initial approximation, and therefore the melting point was used as the initial one. To increase the convergence of the equations set, the method of under-relaxation is used. At the same time, the temperature distribution at each iteration is searched according to the scheme as follows:

$$[T]_n = [T]_{n-1}(1 - \alpha_p) + [T]_n^p \alpha_p, \quad (39)$$

where $[T]_{n-1}$ is the temperature distribution obtained at the previous iteration; $[T]_n^p$ is calculated temperature

distribution at the current iteration obtained by solving the corresponding simultaneous equations; $0 < \alpha_p < 1$ is the relaxation coefficient. At the early iterations, the relaxation coefficient value is selected small $\alpha_p \approx 0.01$, and further it is increased either manually or automatically as the system converges with the use of dependence

$$\alpha_p = \frac{k}{n_i}, \quad (40)$$

where n_i is the number of iterations of the adjoint gradient method when solving a system of equations approximating the heat transfer equation in the reaction zone of the furnace; k is a proportionality coefficient. The use of the results of previous calculations as an initial approximation allows shortening the time for solving a joint system of equations significantly.

To determine the integral characteristics of the reactor volume operating mode, such as full true power, gas output and charge consumption, there is used the provision that the main energy release occurs in the near-electrode areas of the reaction zone. The main part of physico-chemical processes (gas formation and charge melting) also takes place there. In this case, integration is carried out for each electrode by sectors of magnitude ϖ , with the assumption that the heat-evolution on the cylindrical surface equidistant from the electrode is equal to the calculated value at the same distance from the electrode. The value of the total true power in the design section of the furnace bath is determined by the expression

$$P = \iint_S q \pi r_e \delta x \delta y, \quad (41)$$

where q is the specific volumetric energy release; S is the area of the calculated section of the furnace bath; r_e is the distance to the nearest electrode. Integration for three different sections of the furnace allows one to get full power taking into account the electrode interaction with each other at their various deepenings, and, consequently, their positions relative to the bottom. Its value is obtained from the mentioned results for each section and divided by two, since the influence of each electrode is taken into account twice. Similarly, other integral characteristics of the operating mode are determined.

Before starting the computation, the furnace area is divided into superelements and then a grid of finite elements is generated on each of them and, as a result of the combination, a grid of elements for the entire computation area is obtained. After that, arrays are formed to store sets of equations.

The algorithm for calculating heat and mass exchange in an electrothermal ore-smelting reactor is given below:

1. Dividing the computational domain into super-elements for constructing a finite element grid;
2. Constructing a finite element grid;
3. Formation of arrays for storing sets of equations;
4. Formation of simultaneous equations for calculation of electric potential distribution;

5. Calculation of electric potential distribution;
 6. Calculation of the distribution of specific heat-evolution;
 7. Formation of simultaneous equations for calculating the temperature distribution in the melt zone;
 8. Calculation of temperature distribution in the melt zone;
 9. Calculation of the next temperature iteration taking into account the relaxation parameter;
 10. Formation of simultaneous equations for calculating the reagent concentration distribution in the melt zone;
 11. Calculation of the reagent concentration distribution in the melt zone;
 12. Formation of simultaneous equations for calculating the potential function distribution for gas filtration;
 13. Calculation of gas velocity distribution;
 14. Formation of simultaneous equations for calculating the potential function distribution for the charge motion;
 15. Calculation of the potential function distribution for the charge motion;
 16. Calculation of the charge descent rate distribution;
 17. Formation of simultaneous equations for calculating the gas temperature distribution in the furnace charge zone;
 18. Calculation of the gas temperature distribution in the charge-heating zone;
 19. Formation of simultaneous equations for calculating the charge temperature distribution;
 20. Calculation of the charge temperature distribution;
- If convergence was achieved in more than one iteration when performing all calculations, go to step 3;
21. Calculation of integral characteristics of the furnace operation mode.

To implement the model, an integrated environment has been created based on a program using the BorlandC++ 4.5 compiler. That allows calculating the

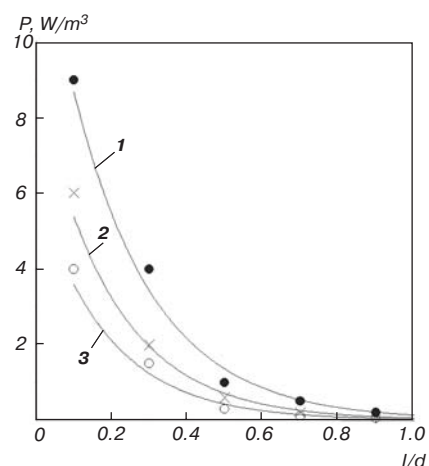


Fig. 2. Distribution of calculated and experimental specific power in OKB-767 furnace bath depending on the distance from the side surface of the electrode: 1, 2, 3 – $\rho_s/\rho_w = 1; 3; 8$ respectively

operating modes of ore-smelting furnaces of any design, including those widely used in non-ferrous metallurgy. The program has a well-developed user interface provided with a menu system, dialog boxes, and a toolbar that allow the user to visualize the results of calculations in the form of isoline fields and velocity vectors (Fig. 4).

As initial data, it is possible to set the geometric dimensions of the furnace: diameter, depth of the bath, diameter of the electrodes and the distance between them, dimensions of the reaction and slag zones; control parameters: position and voltage on the electrodes or the active power of the furnace; conditions of the heat exchange with the environment; thermophysical properties of materials of the calculated zones.

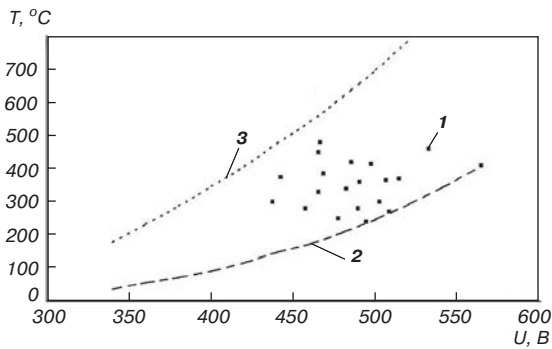


Fig. 3. Calculated and experimental dependences of the waste gas temperature on electrode voltage for RKZ-48F furnace: 1 – experimental data, 2 – calculation at $C_{\kappa} = 12\%$, 3 – calculation at $C_{\kappa} = 8\%$

For adequacy verification of the developed mathematical model, the calculation results of the heat-evolution intensity values have been compared with the data of an electrolytic model experiment. Electrolytic models of the OKB-767 (OKB-767) phosphorus furnace with a capacity of 10 MW have been used in [24–25] as a method of physical modeling of the distribution of electric potential and energy release density in the bath of an ore-smelting phosphorus furnace. A geometrically similar bath has been used, and immiscible electrolytes have been applied to simulate areas with different conductivity. The electric field in the bath has been determined at different values of the conductivity ratio of the working and slag zones ρ_s/ρ_w . The specific volume power has been determined by the electric field measuring results.

The calculations show an acceptable qualitative and quantitative correspondence with the experimental results (Fig. 2).

A sharp decrease in the allocated power depending on the distance to the electrode is characteristic, which entails localization of the target processes in the near-electrode areas.

One of the technological parameters recorded during experiments on operating ore-smelting phosphorus furnaces is the waste gas temperature. This parameter determines the reliability of the furnace roof operation and indirectly characterizes the efficiency of the unit. The results of experimental temperature measurements are within wide limits for the same aggregates, since they are

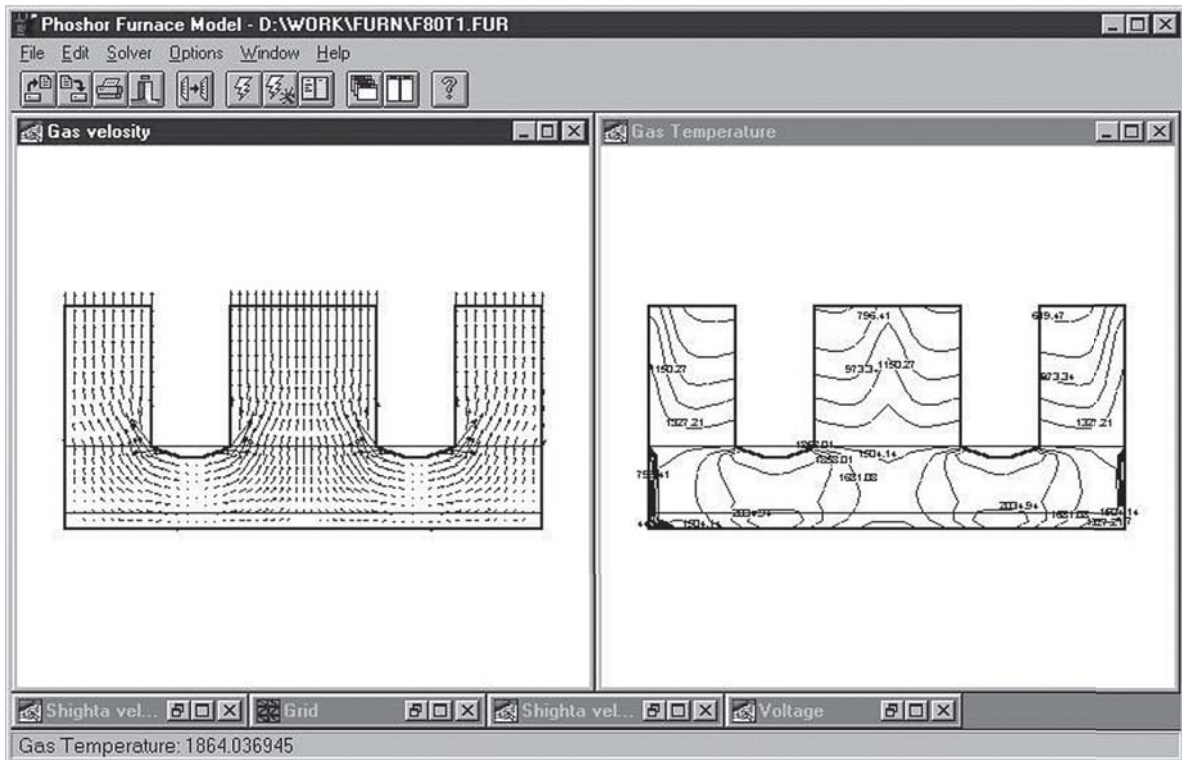


Fig. 4. The appearance of the program interface with the results of computations

determined by a wide range of parameters, most of which are not fixed during the experiment.

Adequacy verification of the mathematical model by the waste gas temperature values has been carried out by comparing the calculation results at different values of electrode voltage and limiting coke dosages in the charge. The results of calculating the outlet temperature for the RKZ-48F (PK3-48Φ) furnaces, compared to the experimental results [13] are shown in Fig. 3. The limiting calculated curves include the gas temperature values in the underroof space, which indicates a qualitative and quantitative correspondence between the model representations and real ore-smelting furnaces.

Comparison of the results shows that the less powerful OKB-640 furnace works more stably and steadily compared to RKZ-48F, since the furnace gas temperature scattering for this type of furnace is smaller and practically not subject to fluctuations when the power is gained and the coke dosage is changed. The temperature dependence on the furnace power has a flat shape, which evidences an inherent regulation of heat exchange processes in this unit.

The program was used to analyze the operating modes of melting furnaces and obtain data on efficiency indicators. Based on the results of calculations, regime maps have been developed, based on which the reactor operation mode is maintained close to optimal, when the specific power consumption is reduced by 2–4%, and, in addition, the time of unplanned equipment downtime is reduced. With the production of one million tons of products per year, the annual economic effect at the minimum tariff will be approximately 1 billion rubles without additional capital investments.

Conclusions

1. The proposed model and the developed algorithm make it possible to use the program to calculate the distribution of electric potential, specific energy release, material temperature, gas temperature, reagent concentration in the reaction zone, presented in the form of isoline fields and the distribution of gas velocity and charge descent rate, presented in the form of vector fields, as well as the values of integral characteristics of the furnace bath operating mode, such as an true electric power, gas output, consumption of individual charge components, average and maximum gas temperatures at the furnace outlet, allowing to evaluate the performance indicators of reduction reactors of non-ferrous metallurgy as well.

2. The developed program makes it possible to calculate the mode maps to control the parameters that ensure optimal operating modes.

The work was carried out as part of the State task, project No. FSWF-2020-0019.

References

1. Mikulinsky A. S. Parameters Determination of Ore-Thermal Furnaces Based on the Similarity Theory. Moscow: Energiya, 1964. 260 p.
2. Chumakov Yu. A., Mazmanyany V. A., Rumyantsev D. V., Tsemekhman L. Sh., Egorov P. A. Analysis of Ore-Thermal Furnace Operation at "Pechenganickel" Combine Under Conditions of Changing of Charge Composition. *Tsvetnye Metally*. 2014. No. 1. pp. 35–40.
3. Kondreshev V. P., Mironov Yu. M., Kozlov A. I. et al. Study of the Operating Modes of Industrial Electric Furnaces for Calcium Carbide Production. *Ore-smelting electric furnaces: collection of scientific works*. Moscow: Energoatomizdat, 1988. pp. 32–38.
4. Nekhamin S. M. Band Structure of Bath of Electrode Smelting Furnaces at Operation on DC and Underfrequency Current. *Metallurgist*. 2014. No. 2. pp. 57–64.
5. Hariharan M., Rafi K. Mohd., Raghavan D. Modelling of Calcium Carbide Furnace. *Bulletin of Electrochemistry*. 1990. Vol. 6, Iss. 3. pp. 298–301.
6. Yang Y., Xiao Y., Reuter M. Analysis of Transport Phenomena in Submerged Arc Furnace for Ferrochrome Production. *Tenth International Ferroalloy Congress, INFACONX: Transformation through Technology, 1–4 February 2004, Cape Town, South Africa*. pp. 15–25.
7. Scheepers E., Yang Y., Adema A. T., Boom R., Reuter M. A. Process Modeling and Optimization of a Submerged Arc Furnace for Phosphorus Production. *Metallurgical and Materials Transactions B*. 2010. Vol. 41, No. 5. pp. 990–1005.
8. Rumyantsev D. V., Talalov V. A., Stepanov V. V., Rusaikov M. R. Simulation of the Mass and Heat Transfer Processes in a Three-Electrode Round Depletion Furnace. *Technology and Equipment of Ore-Smelting Production: Collection of Works of Scientific and Technical Conference with International Participation "Electrothermia-2008"*. St. Petersburg, 2008. pp. 175–187.
9. Pancnezhko S. V., Dli M. I., Borisov V. V., Panchenko D. S. Analysis of Thermalphysic Processes in Near-Electrode Zone of Electrothermal Reactor. *Non-ferrous Metals*. 2016. No. 2. pp. 57–64. DOI: 10.17580/nfm.2016.12.12.
10. Panchenko S. V., Dli M. I., Bobkov V. I., Panchenko D. S. Problems of Analysis of Thermalphysic Processes in a Reaction Zone of Electrothermal Reactor. *Non-ferrous Metals*. 2017. No. 1. pp. 36–42. DOI: 10.17580/nfm.2017.01.08
11. Puchkov A. Yu., Lobaneva E. I., Kulygin O. P. Algorithm for Predicting the Parameters of a System for Processing Waste Apatite-Nepheline Ores. *Journal of Applied Informatics*. 2022. Vol. 17, No. 1. pp. 55–68.
12. Dli M. I., Vlasova E. A., Sokolov A. M., Morgunova E. V. Creation of a Chemical-Technological System Digital Twin Using the Python Language. *Journal of Applied Informatics*. 2021. Vol. 16, No. 1. pp. 22–31.
13. Zhilov G. M., Valkova Z. A., Tarasov V. A., Tavrin N. Yu. Effect of Electrical Processing Regime on the Parameters of the Phosphorus Furnace Gas. *Sovershenstvovanie Protsssov i Apparatov Proizvodstva Karbida Kaltsiya, Fosfora i Fosfornykh Solei*. Leningrad: LenNIIGiproKhim, 1988, pp. 93–103.

14. Panchenko S. V., Panchenko D. S., Glebova N. B. Transfer Processes in Heterogeneous Reduction Reactors. *Theoretical Foundations of Chemical Engineering*. 2004. Vol. 38, Iss. 6. pp. 611–615.
15. Huyakorn P. S. Solution of Steady-State, Convective Transport Equation Using an Upwind Finite Element Scheme. *Applied Mathematical Modelling*. 1977, Vol. 1, Iss. 4. pp. 187–195.
16. Hasbani Y., Engelman M. Out-of-Core Solution of Linear Equations with non-Symmetric Coefficient Matrix. *Computers & Fluids*. 1979. Vol. 7, Iss. 1. pp. 13–31.
17. Yanenko N. N., Danaev N. T., Liseikin V. D. A variational method for grid generation. *Chislennye Metody Mekhaniki Sploshnoi Sredy*. 1977. Vol. 8, Iss. 4. pp. 157–163.
18. George A., Liu J. W.-H. Computer Solution of Large Sparse Positive Definite Systems. Transl. from Eng. by Kh. D. Ikramov. Moscow: Mir, 1984. 333 p.
19. Kuznetsov Yu. A. Computational Methods in Subspaces. *Computational Processes and Systems*. Iss. 2. Moscow : Nauka, 1985. pp. 265–350.
20. Marchuk G. I., Kuznetsov Yu. A., Iterative Methods and Quadratic Functionals. Novosibirsk: Nauka, Sibirskoye otdele-niye, 1972. 205 p.
21. Polezhaev V. I., Prostomolotov A. I., Fedoseev A. I. Finite Element Method in Viscous Fluid Mechanics. *Itogi nauki i tekhniki VINITIAN SSSR. Seriya: Mekhanika zhidkosti i gasa*. 1987. Vol. 21. pp. 3–92.
22. Tesser R., Santacesaria E. Revisiting the Role of Mass and Heat Transfer in Gas–Solid Catalytic Reactions. *Processes*. 2020. Vol. 8, Iss. 12. p. 1599.
23. Hu H.-P. Theoretical Study of Convection Heat Transfer and Fluid Dynamics in Microchannels with Arrayed Microgrooves. *Mathematical Problems in Engineering*. Vol. 2021. pp. 1–12.
24. Valkova Z. A., Dantsis Ya. B., Zhilov G. M., Antonos E. R. Electric Field in the Phosphorus Furnace Bath. *Issledovanie i razrabotka elektrooborudovaniya i sistem avtomaticheskogo upravleniya moshchnykh rudnotermicheskikh pechei*. 1975. Iss. 20. pp. 34–41.
25. Zhilov G. M., Valkova Z. A., Dressen V. V. Methodical Recommendations on the Determination of Energy Distribution in Baths of Chemical Electrothermal Furnaces. Leningrad : LenNII GiproKhim, 1985. 32 p.